A dynamic localization of 2D electrons at mesoscopic length scales

A. Ghosh, M. Pepper, H. E. Beere, D. A. Ritchie

Cavendish Laboratory, University of Cambridge, Madingley Road, Cambridge CB3 0HE, United Kingdom
(Dated: February 2, 2008)

We have investigated the local magneto-transport in high-quality 2D electron systems at low carrier densities. The positive magneto-resistance in perpendicular magnetic field in the strongly insulating regime has been measured to evaluate the spatial concentration of localized states within a mesoscopic region of the samples. An independent measurement of the electron density within the same region shows an unexpected correspondence between the density of electrons in the metallic regime and that of the localized states in the insulating phase. We have argued that this correspondence manifests a rigid distribution of electrons at low densities.

The nature of localization of electrons in low dimensional systems is a matter of continuing debate. The enhanced effect of Coulomb interaction in such systems gives rise to quantum many-body ground states which, depending on the extent of disorder, may display a wide variety of excitation spectra and real-space distribution of charge. From extensive theoretical [1] and experimental [2] investigations, it is now generally agreed that at zero temperature ($T = 0$), a gap would appear in the single particle density-of-states (DOS) at the Fermi energy (E_F), even though the form of this gap remains controversial. On the other hand, direct experimental determination of the spatial distribution of the localized states is significantly rare. Theoretically, several forms of the distribution have been predicted in the absence of disorder, which include Wigner crystals [3], bubbles or striped phases [4]. However, when disorder is present, strong localization is associated with the pinning of electrons to a static, randomly distributed impurity sites. In this paper, we have addressed this issue by directly probing the spatial distribution of localized states within a mesoscopic region of low-density 2D electron systems (2DES) at various levels of background disorder. We find that even in the strongly insulating regime, the areal density of these states (n_L) changes with the electron density (n_s), and hence are "dynamic" in nature. When analyzed in the framework of percolation theory, a direct correspondence between n_L and n_s could be established, implying an unexpected rigid distribution of the electrons that is independent of the topology of background disorder, but depends only on E_F of the system.

In disordered 2DES, the strongly localized regime is identified by a longitudinal resistivity $\rho \gg h/e^2$, and an activated (nearest-neighbor) hopping or a variable-range hopping transport, where $\rho(T) \sim \rho_0 \exp{(T_0/T)^p}$, T_0 and p being the relevant energy scale and hopping exponent respectively. In a weak magnetic field (B), applied perpendicular to the plane of the 2DES, the asymptotic behavior of the wave-function of an isolated impurity state changes to $\psi(r) \sim \exp{(-r/\xi - r^3\xi/24\lambda^4)}$, where ξ is the localization length and $\lambda = \sqrt{\hbar/eB} \gg \xi$ [5]. The

B-induced compression of the wave-function leads to a strong positive magneto-resistance (MR), which is expressed analytically as $\rho(T, B) = \rho(T, B = 0) \exp{(\alpha B^2)}$. An expression for the geometry-dependent factor α has been derived from the shift in percolation threshold, which in the limit of narrow bandwidth can be expressed as [6],

$$\alpha \approx A_L \frac{e^2 \xi}{\hbar^2 n_L^{3/2}}, \qquad (1)$$

where A_L is a model-dependent constant of order unity, whose precise value will be discussed later. Eq. 1 provides a mechanism of estimating n_L from the weak-field MR in strongly localized systems, and has been used in the context of hopping transport in the impurity band of δ-doped GaAs [7]. In the present work we have used this technique to calculate n_L within a mesoscopic area in low-disorder 2DES, and compared it to the absolute value of n_s within the same region.

As shown in the schematic of Fig. 1a, mesoscopic segments of high-mobility Si δ-doped GaAs/AlGaAs heterostructures were created by the intersection of a narrow wet-etched mesa (width: W) and a transverse Au/NiCr metallic gate (width: L). The doping density $n_\delta = 2.5 \times 10^{12}$ cm^{-2} was kept constant for all samples, while the background disorder was tuned by changing the separation (δ_{sp}) of the dopant layer and the GaAs-AlGaAs interface. The value of n_s within the active region depends on the gate voltage (V_g) through the specific capacitance C_0. Within the simple capacitor model, $C_0 \simeq \epsilon_0\epsilon_r/ed_s$, where d_s is the depth of the 2DES from the surface. For this experiment we have chosen mesoscopic samples from two heterostructures, which differ in δ_{sp} and d_s, but identical in all other structural and geometrical aspects. The relevant parameters are given in Table I. Note that sample A07 is more disordered than A78 due to a smaller δ_{sp}, and hence has lower electron mobility (μ). All experiments were performed at $T \approx 0.3$ K unless specified otherwise. In order to minimize the effect of contact and series resistances, the electrical measurements were car-

TABLE I: Relevant parameters of the samples used. $\mu(0)$ and $n_s(0)$ are as-grown mobility and electron density respectively.

Sample	$\mu(0)$ cm^2/V-s	$n_s(0)$ cm^{-2}	δ_{sp} nm	d_s nm	$L \times W$ μm$\times\mu$m	C_0 cm^{-2}V^{-1}
A07	0.6×10^6	2.9×10^{11}	20	120	2×8	57×10^{10}
A78	1.8×10^6	2.1×10^{11}	40	290	2×8	24×10^{10}

ried out only in 4-probe geometry with a low-frequency (~ 7.2 Hz) ac excitation current of $\sim 0.01 - 0.1$ nA. The maximum measured resistance was limited to ~ 1.5 MΩ to avoid any systematic error arising from stray capacitances.

The first part of the experiment evaluates the V_g−dependence of n_s when n_s is sufficiently high such that $\rho \ll h/e^2$ and quantum Hall-based methods are applicable. However, due to the restricted dimensions of the active region, in particular the smallness of L, conventional Hall or Shubnikov-de Haas measurements are experimentally unfeasible in these samples. Hence, we have used an alternative technique based on the reflection of edge-states, which was originally developed to study backscattering of edge-states by well-defined potential barriers [8]. The technique is schematically represented in Fig. 1a. Briefly, when the perpendicular B corresponds to ν_0 edge channels in the ungated part of the Hall-bar, a negative V_g will cause $\nu_0 - \nu$ of the channels to get reflected at the gate, where ν is the filling factor within the active region. As a function of V_g, this leads to plateaus in the four-probe resistance ($R_{12,34}$) at $R_{12,34} = (h/e^2)(1/\nu - 1/\nu_0)$, when the contacts (1-4) in Fig. 1a are close to ideal with no reflection and perfect transmission. This is illustrated in Fig. 1b, where the V_g−dependence of $R_{12,34}$ is measured in sample A78 at a constant B corresponding to $\nu_0 = 10$. Three plateaus corresponding to $\nu = 8$, 6 and 4 appear nearly exactly at the theoretically expected values (horizontal dashed lines). The V_g at the center of these plateaus then corresponds to an electron density of $n_s = eB\nu/h$, while the width of the plateau represents the maximum uncertainty. For both samples, we have repeated this measurement for different values of ν_0 (within spin degeneracy).

Fig. 1c shows n_s as a function of V_g for samples A07 (empty symbols) and A78 (filled symbols). An advantage of this method is the negligible uncertainty in the y-direction since n_s is derived from a known integer (ν). At a sufficiently negative V_g both samples display the expected linear dependence of n_s on V_g. In A07, the deviation from linearity at higher V_g can be explained from screening of V_g by accumulation of carriers in the dopant layer [9]. When the linear part is fitted with $n_s = C_s(V_g - V_{gs}^0)$, the slope C_s was found to be $\approx 55.5 \times 10^{10}$ cm^{-2}V^{-1} for A07 and $\approx 23.0 \times 10^{10}$ cm^{-2}V^{-1} for A78, agreeing satisfactorily with corresponding values of C_0. The intercept V_{gs}^0 was found to be $V_{gs}^0 = -0.917 \pm 0.004$

V and -0.804 ± 0.002 V for A07 and A78 respectively.

We now consider the strongly localized regime, where $\rho \gg h/e^2$. As shown in the insets of Fig. 2, at $B = 0$, this regime corresponds to $V_g \lesssim -0.86$ V for A07 and $V_g \lesssim -0.74$ V for A78. Increasing B from zero initially results in some negative MR in both samples, followed by an exponential rise in $\rho(B)$ at higher B. The dependence of $\ln \rho$ on B^2 at different V_g for both samples is shown in Fig. 2. In order to ensure consistency, the analysis is limited to the regime of V_g for which $\rho(B = 0) \gtrsim 2h/e^2$. From Fig. 2, within the measured range of ρ, $\ln \rho$ varies linearly with B^2 over a field range of 1.2 T $\lesssim B \lesssim 3$ T for A07 and 0.5 T $\lesssim B \lesssim 1.3$ T for A78. The lower limit of B is determined by the extent of negative MR, which arises from an interference among the hopping paths [10]. The upper cut-off in B probably arises from the strong-field condition $r \ll \lambda^2/\xi$ for the asymptotic form the wave-function $\psi(r)$ [5]. This is not fully understood at present and will be discussed in a future publication.

The most striking aspect of the data shown in Fig. 2 is the continuous decrease in the slope α of $\ln \rho - B^2$ traces as V_g is made more positive (i.e. as n_s is increased). This is observed in both samples (Fig. 3). Note that from the expression for α in conventional hopping framework (Eq. 1), α is expected to increase with increasing V_g since the localization length ξ increases rapidly as the system becomes more metallic (n_L remains constant since it is assumed to arise from frozen impurity distribution). This has been confirmed in hopping MR in the Na$^+$ impurity band of Si-MOSFET's, where α was found to increase as the Fermi energy was swept towards band half-filling [11]. In our case, we also note that the absolute magnitude of α is about factor of ~ 2 larger in A78 than A07 over the same range of ρ.

If we assume the validity of Eq. 1, the counter-intuitive trend of α in Fig. 3 forces n_L to be V_g-dependent. Following Ref. [7], since $\rho \gg h/e^2$, we first replace ξ of the hydrogenic wave-function of the strongly localized states by a_B^*, where a_B^* is the effective Bohr radius of electrons. However, an evaluation of n_L from Eq. 1 also requires the magnitude of A_L. If the system consists of only two isolated localized states, one obtains A_L simply from the overlap integral as $A_L = 1/12 \approx 0.083$ [12]. However, in the hopping regime there are a large number of states, and the relation $A_L = (N_c/\pi)^{3/2}/12$ can be obtained following Nguen's analysis of the B-induced shift in percolation threshold. Here N_c is the dimensionality-dependent number of bonds per site in the random resistor network [6]. $N_c = 4.5$ or 2.7, for zero or finite width of the impurity band with respect to $k_B T$ [11, 13]. This gives $A_L \approx 0.143$ and 0.0664 respectively. Note that all the estimates of A_L are well within the order of unity, and hence only has a fine tuning effect on the absolute magnitude of n_L. In the subsequent analysis we have used $A_L = 0.0664$, even though the effect of other values of A_L has also been discussed.

Fig. 4a shows the V_g−dependence of n_L evaluated using Eq. 1 and the experimentally obtained α. Note that for both samples n_L displays an approximately linear dependence on V_g. A fit of the form $n_L = C_L(V_g - V_{gL}^0)$ gives $C_L \approx 55.7 \times 10^{10}$ cm^{-2}V^{-1} and 23×10^{10} cm^{-2}V^{-1}, and $V_{gL}^0 \approx -0.918 \pm 0.003$ V and -0.806 ± 0.005 V for A07 and A78 respectively.

The calibration of n_s with V_g now allows us to identify an unexpected correspondence between n_L and n_s for both samples. Firstly, the slopes C_s and C_L agree with each other as well as the expected specific capacitance C_0. Secondly, the pinch-off voltages V_{gL}^0 and V_{gs}^0 are also equal within the experimental accuracy. To confirm this correspondence, we have plotted n_L and n_s together as functions of ΔV_g, where $\Delta V_g = V_g - V_{gL}^0$ for n_L and $V_g - V_{gs}^0$ for n_s. Fig. 4b clearly shows n_L to be a continuation of n_s in the low-density, strongly-localized regime in both samples. While the best alignment could be obtained using $A_L = 0.0664$, Fig. 4b also illustrates the position of n_L relative to n_s for A07 with $A_L = 0.143$ (dotted line) and $A_L = 0.083$ (dashed line).

The correspondence between n_L and n_s clearly demonstrates a distribution of localized states that is independent of the topology of disorder, but depends only on the density of electrons. Such a possibility has been discussed extensively in the context of Wigner crystallization in low-density systems. Recent quantum Monte Carlo simulations have indicated the possibility of stabilizing a Wigner-like rigid distribution of electrons at relatively high electron densities in presence of optimum disorder [14]. Microwave absorption studies have also claimed possible observation of Wigner solid in the fractional quantum Hall regime at n_s as high as $\sim 6 \times 10^{10}$ cm^{-2} [15]. Transport in such systems has been discussed in terms of hopping of vacancies or interstitials, or the excitation of such species to the mobility edge [16, 17]. In this experiment, even though we have probed the spatial distribution of localized states in a more direct manner, we cannot, at least at present, make a definite statement on any order in the distribution. This would require further understanding of the geometrical parameters, in particular A_L, which is presently under investigation.

The temperature dependence of α provides further insight to the nature of the "impurity" band and corresponding DOS (D_L). In the inset of Fig. 3b we have shown a typical T−dependence of α, corresponding to $V_g = -0.760$ V for A78. Over the observed range of T, α is nearly constant. In the percolation framework, this confirms the validity of Eq. 1 for our system and allows us to express the bandwidth W as $W \lesssim k_B T \ln(\eta_c)$, where η_c determines the resistivity at the percolation threshold, $\rho = \rho_0 \exp(\eta_c)$. To get an estimate of W, we use the observed $\rho/\rho_0 \approx 6$ at $V_g = -0.76$ V and $T = 0.3$ K. ($\rho_0 \sim h/e^2$ was obtained from T−dependence of ρ.) This gives $W \lesssim 0.05$ meV, and from the observed $n_L \approx 1 \times 10^{10}$

cm^{-2} at the same V_g, we get $D_L \sim n_L/W \approx 2.1 \times 10^{14}$ cm^{-2}eV^{-1}. Interestingly, this is nearly an order of magnitude larger than even the spin-degenerate free-electron DOS in GaAs, $m^*/\pi\hbar^2 = 2.7 \times 10^{13}$ cm^{-2}eV^{-1}. Similar observation was reported in the context of transport near the mobility edge in the inversion layer of Si-MOSFETs [18]. While a shift in the mobility edge as a function of E_F was suggested, in our case possibility of an interaction-induced enhancement of the effective mass (m^*) cannot be ruled out.

An important aspect of the solid phase is the spin of individual localized states. Rigid electronic distribution at n_L as large as $1 - 5 \times 10^{10}$ cm^{-2} will definitely involve strong exchange interaction. Both ferromagnetic and anti-ferromagnetic ground states have been predicted depending on the nature of ring exchange in this phase [16, 19]. Indeed, possible observation of a spontaneously spin-polarized phase, in particular at lower dimensions, is now being reported in several experimental investigation in the low-density regime [16, 20].

In conclusion, magneto-transport in the strongly localized, low-density regime of high-quality 2D electron systems provide evidence of a dynamic, gate voltage-dependent distribution of localized states. Over a mesoscopic region of the 2D systems, the spatial density of the localized states was found to agree with the estimated density of electrons at the same gate voltage. This correspondence is argued to be manifestation of a many-body rigid distribution of electrons, driven by strong Coulomb interaction.

[1] N. F. Mott and E. A. Davis, in *Electronic Processes in Non-Crystalline Materials* (Claredon Press, Oxford, 1979); A. L. Efros and B. I. Shklovskii, J. Phys. C: Solid State Phys. **8**, L49 (1975); A. Perez-Garrido, M. Ortuno, E. Cuevas, J. Ruiz and M. Pollak, Phys. Rev. B **55**, R8630 (1997).
[2] F. Tremblay *et al.*, J. Phys. Condens. Matter **2** 7367 (1990); W. Mason *et al.*, Phys. Rev. B **52**, 7857 (1995); F. W. Van Keuls, X. L. Hu, H. W. Jiang and A. J. Dahm, Phys. Rev. B **56**, 1161 (1997); E. Bielejec and W. Wu, Phys. Rev. Lett. **87**, 256601 (2001).
[3] B. Tanatar and D. M. Ceperley, Phys. Rev. B **39**, 5005 (1989).
[4] A. A. Koulakov, M. M. Fogler and B. I. Shklovskii, Phys. Rev. Lett. **76**, 499 (1996); A. A. Slutskin, V. V. Slavin and H. A. Kovtun, Phys. Rev. B **61**, 14184 (2000).
[5] B. I. Shklovskii, Sov. Phys. Semicond. **17**, 1311 (1983); B. I. Shklovskii and A. L. Efros, in *Electronic Properties of Doped Semiconductors*, Vol. 45 of Springer Series in Solid-State Sciences (Springer, Berlin, 1984).
[6] V. L. Nguen, Sov. Phys. Semicond. **18**, 207 (1984).
[7] Q. Y. Ye, B. I. Shklovskii, A. Zrenner, F. Koch and K. Ploog, Phys Rev. B **41**, 8477 (1990).
[8] R. J. Haug, A. H. MacDonald, P. Streda and K. von Klitzing, Phys. Rev. Lett. **61**, 2797 (1988); S. Washburn,

A. B. Fowler, H. Schmid and D. Kern, *ibid.* **61**, 2801 (1988).

[9] K. Hirakawa, H. Sakaki and J. Yoshino, Appl. Phys. Lett. **45**, 253 (1984).

[10] W. Schirmacher, Phys. Rev. B **41**, 2461 (1990); V. L. Nguen, B. Z. Spivak and B. I. Shklovskii, Sov. Phys. JETP **62**, 1021 (1986).

[11] G. Timp and A. B. Fowler, Phys. Rev. B **33**, 4392 (1986).

[12] A. K. Savchenko *et al.*, Phys. Rev. B **52**, R17021 (1995).

[13] P. N. Butcher and K. J. Hayden, Phil. Mag. **36**, 657 (1977).

[14] S. T. Chui and B. Tanatar, Phys. Rev. Lett. **74**, 458 (1995).

[15] P. D. Ye *et al.*, Phys. Rev. Lett. **89**, 176802 (2002).

[16] T. Okamoto and S. Kawaji, Phys. Rev. B **57**, 9097 (1998).

[17] E. Cockayne and V. Elser, Phys. Rev. B **43**, 623 (1991).

[18] M. Pepper, S. Pollitt and C. J. Adkins, J. Phys. C: Solid State Phys. **7**, L273 (1974).

[19] M. Roger, J. H. Hetherington and J. M. Delrieu, Rev. Mod. Phys. **55**, 1 (1983).

[20] K. J. Thomas *et al.*, Phys. Rev. Lett. **77**, 135 (1996); A. A. Shashkin *et al.*, *ibid.* **87**, 086801 (2001); A. Ghosh *et al.*, cond-mat/0310628; *To appear in* Phys. Rev. Lett. (2004).
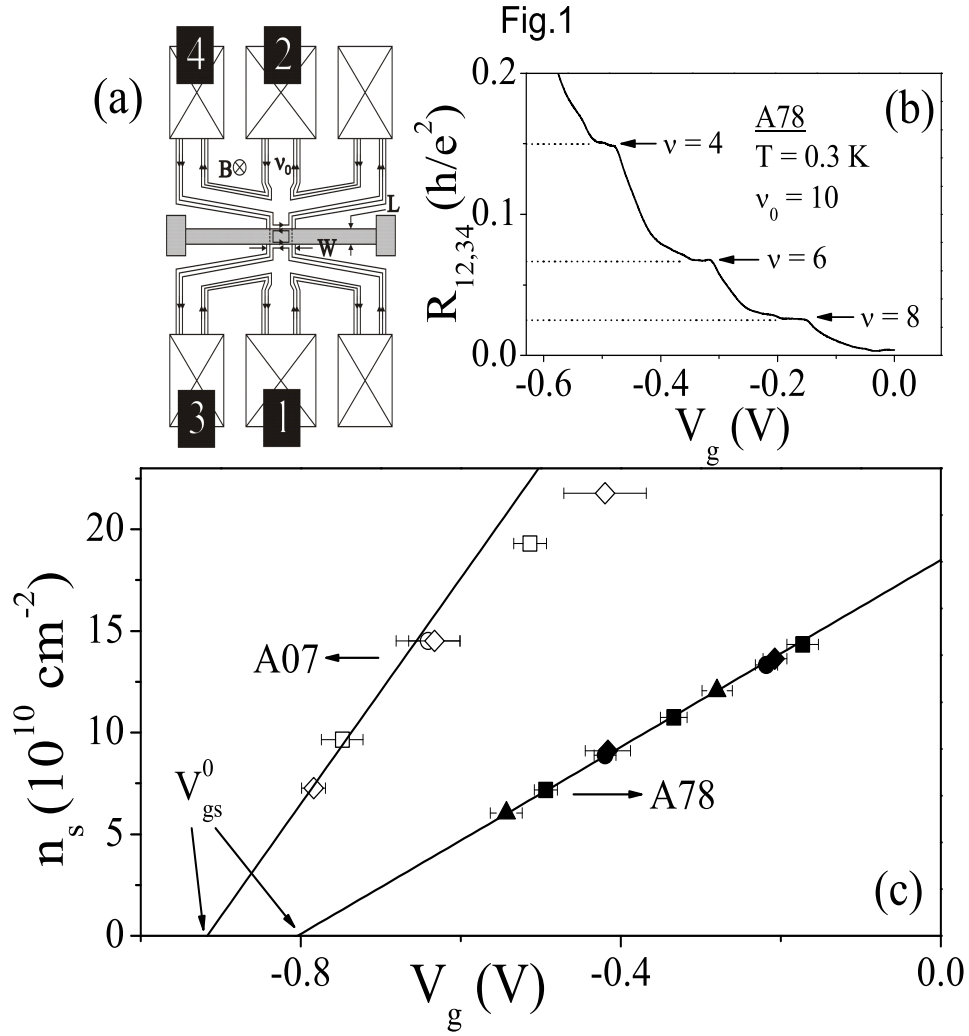
Fig.1

FIG. 1: (a) A schematic of the device structure. Contacts 1 and 2 are for current probes, while 3 and 4 used for voltage probes. (b) Illustration of gate voltage (V_g) dependence of the 4-probe resistance $R_{12,34}$ at a constant magnetic field ($B = 0.742$ T) corresponding to an integral filling factor ν_0 (= 10) in sample A78. The dashed lines are the expected values of $R_{12,34}$ at different filling factors ν within the gated region (see text). (c) $n_s = eB\nu/h$, at values of V_g's corresponding to the center of plateaus in $R_{12,34}$. The horizontal error bars represent the width of the plateaus in V_g. The solid lines are fits to the linear part of the data. For both samples, different symbols correspond to different integral value of ν_0 at which $R_{12,34} - V_g$ sweeps were recorded.
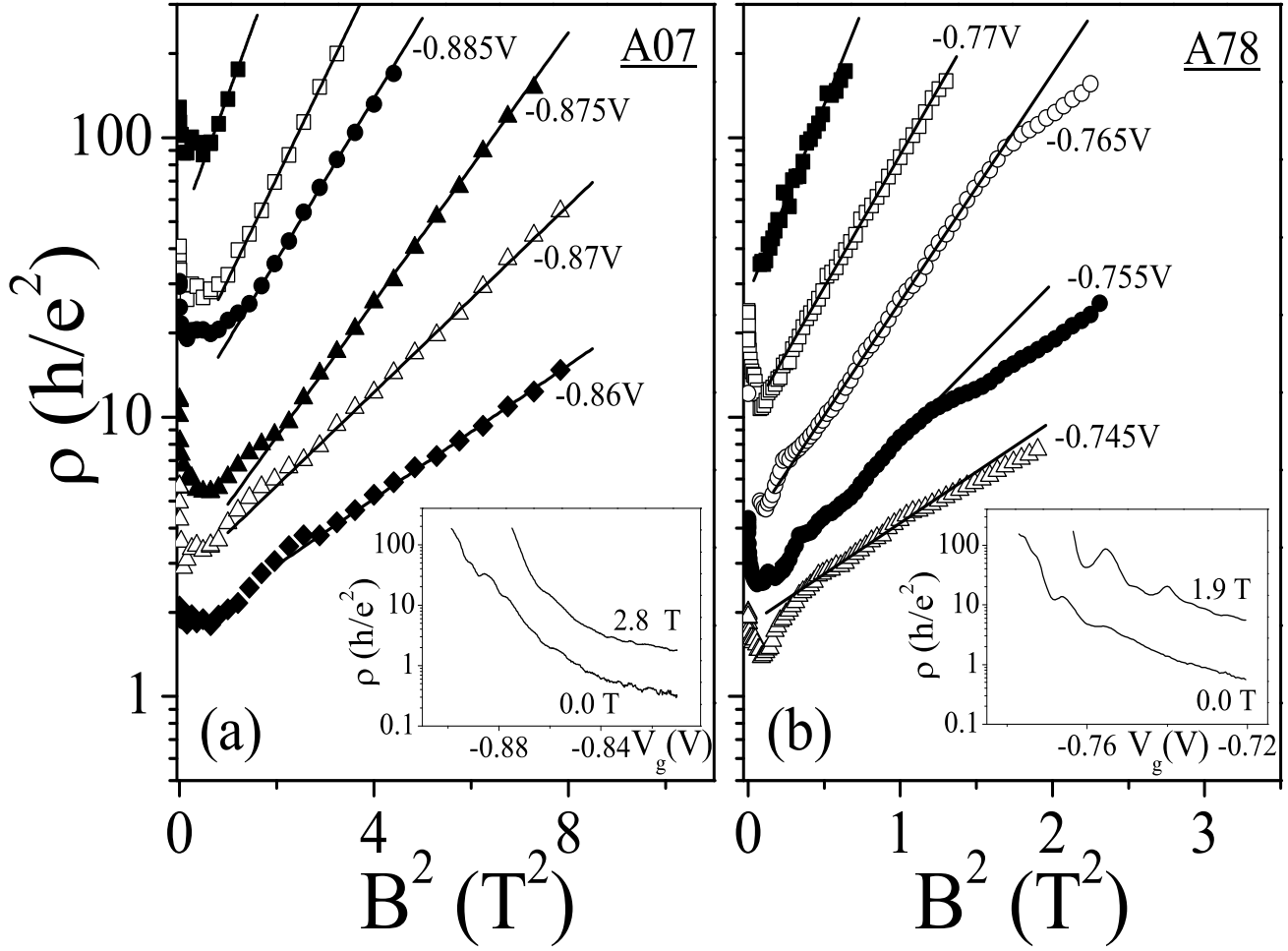
Fig.2

FIG. 2: Dependence of resistivity ρ on B^2 for different values of gate voltage (V_g) recorded at $T = 0.3$ K. Inset: V_g-dependence of ρ at zero and finite B. (a) Sample A07, and (b) Sample A78.
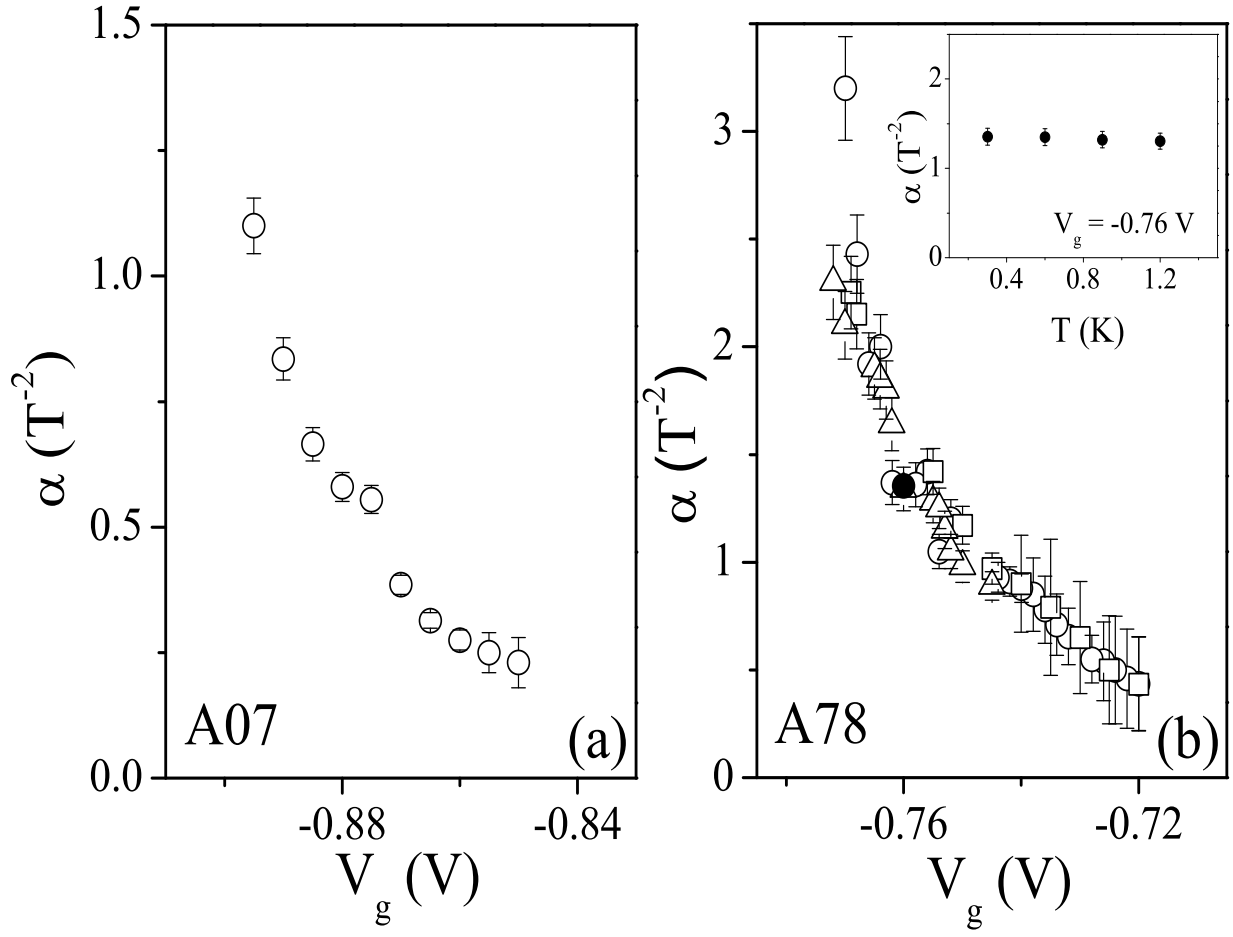
Fig.3

FIG. 3: Gate voltage (V_g) dependence of the slope (α) of the linear region of $\ln(\rho) - B^2$ data shown in Fig. 2. The data was obtained at $T = 0.3$ K. The fit uncertainty increases, and hence the error bar on α, as ρ decreases to $\sim h/e^2$. (a) Sample A07, and (b) Sample A78. Inset of (b): the typical temperature dependence of α obtained at $V_g = -0.760$ V for A78.
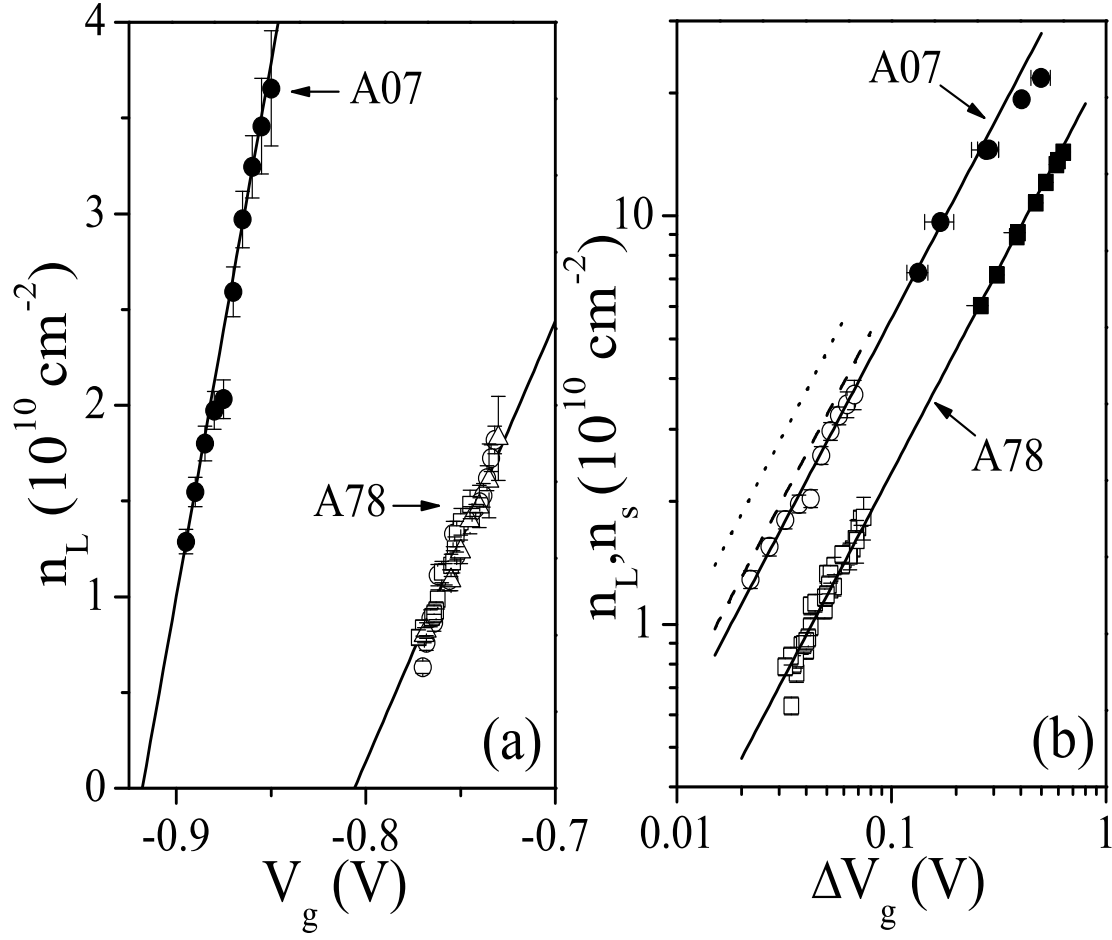
Fig.4

FIG. 4: (a) The spatial density of localized states (n_L) as a function of V_g calculated from Eq. 1 and the experimentally obtained α. Solid lines denote linear fit. (b) Correspondence between n_L and n_s. For comparison, n_L, $n_s - \Delta V_g$ are plotted in log-log scale, where $\Delta V_g = V_g - V_{gL}^0$ for n_L (empty symbols) and $V_g - V_{gs}^0$ for n_s (filled symbols). For A07, the solid, dashed and dotted lines represent estimates of n_L assuming $A_L = 0.0664, 0.083$ and 0.143 respectively.